International Journal of Pharmaceutics 404 (2011) 57–65

Contents lists available at ScienceDirect

International Journal of Pharmaceutics

journal homepage: www.elsevier.com/locate/ijpharm

Preparation and characterization of directly compactible layer-by-layer nanocoated cellulose

Schalk J. Strydom[a], Daniel P. Otto[a], Wilna Liebenberg[b], Yuri M. Lvov[c], Melgardt M. de Villiers[a,*]

[a] School of Pharmacy, University of Wisconsin-Madison, 777 Highland Avenue, Madison, WI 53705-2222, USA
[b] Unit for Drug Research and Development, Faculty of Health Sciences, North-West University, Potchefstroom 2520, South Africa
[c] Institute for Micromanufacturing and Biomedical Engineering Program, Louisiana Tech University, Ruston, LA 71272, USA

ARTICLE INFO

Article history:
Received 15 July 2010
Received in revised form 22 October 2010
Accepted 30 October 2010
Available online 5 November 2010

Keywords:
Layer-by-layer
Self-assembling
Nanocoating
Cellulose
Direct compression

ABSTRACT

Microcrystalline cellulose is a commonly used direct compression tablet diluent and binder. It is derived from purified α-cellulose in an environmentally unfriendly process that involves mineral acid catalysed hydrolysis. In this study Kraft softwood fibers was nanocoated using a layer-by-layer self-assembling process. Powder flow and compactibility results showed that the application of nano-thin polymer layers on the fibers turned non-flowing, non-compacting cellulose into powders that can be used in the direct compression of tablets. The powder flow properties and tableting indices of compacts compressed from these nanocoated microfibers were similar or better than that of directly compactible microcrystalline cellulose powders. Cellulose microfibers coated with four PSS/PVP bilayers had the best compaction properties while still producing tablets that were able to absorb water and disintegrate and did not retard the dissolution of a model drug acetaminophen. The advantages of nanocoating rather than traditional pharmaceutical coating are that it add less than 1% to the weight of the fibers and allows control of the molecular properties of the surface and the thickness of the coat to within a few nanometers. This process is potentially friendlier to the environment because of the type and quantity of materials used. Also, it does not involve acid-catalyzed hydrolysis and neutralization of depolymerized cellulose.

1. Introduction

Tablets, and in particular directly compressed tablets, are considered to be the most desirable dosage form for drug delivery since it is affordable and convenient for patients, and it has a straightforward, easily controllable and low cost manufacturing process which is attractive for pharmaceutical manufacturers and friendlier to the environment (De la Luz Reus Medina and Kumar, 2007; McCormick, 2005). Also, the process of direct compression consists of only two manufacturing steps including mixing of the constituent powders and compression to produce the final tablet dosage form, and this is beneficial in the pharmaceutical industry since it reduces the risk that an error may be introduced during the manufacturing process which could compromise the safety and stability of the final product (McCormick, 2005).

Most dosage forms require the addition of excipients in order to assist in the manufacture and delivery of the dosage form, and for directly compressed tablets these include diluents, binders, lubricants, disintegrants and glidants (Aulton, 2000; De la Luz Reus Medina and Kumar, 2006; Peck et al., 1989). Cellulose fibers, manufactured from the purification and size reduction of α-cellulose fibers from the pulp of fibrous plant materials, serves as the basis for the manufacture of a variety of these excipients but it is not used in its unmodified form due to its poor flow properties (Aulton, 2000; De la Luz Reus Medina and Kumar, 2007). A modified cellulose, microcrystalline cellulose (MCC) is the most commonly used diluent or binder in directly compressed tablets. MCC is derived from purified wood α-cellulose by the treatment of the cellulose fibers with mineral acids (De la Luz Reus Medina and Kumar, 2006; Doelker, 1993). This acid treatment results in the hydrolysis of the amorphous cellulose fibers which also reduces the degree of polymerization in the cellulose chains, and this leads to the formation of aggregates of microcrystals with an average particle size in the micrometer range (Chuayjuljit et al., 2008; Doelker, 1993). The reason for this modification is that the unmodified cellulose fibers have poor flow and compression properties compared to MCC, and these two properties play an essential role in the manufacturing of tablets through direct compression since it influences the weight uniformity, compressibility and tensile strength of the tablets (Lindner and Kleinebudde, 1994). However the process through which MCC is manufactured is environmentally unfriendly since it consumes large quantities of fresh water which is difficult to recycle as a result of the treatment with strong mineral acids. More environmentally friendly methods for preparing MCC have been suggested

* Corresponding author. Tel.: +1 608 890 0732; fax: +1 608 262 5345.
E-mail address: mmdevilliers@pharmacy.wisc.edu (M.M. de Villiers).

0378-5173/$ – see front matter © 2010 Elsevier B.V. All rights reserved.
doi:10.1016/j.ijpharm.2010.10.056

(Chuayjuljit et al., 2008; Stupińska et al., 2007). There are two possible options available in order to be more environmentally conscious during the manufacturing of directly compressed tablets, and these are to either develop another environmentally friendly method for the production of MCC, or to develop method of altering the flow and compression properties of the unmodified cellulose fibers in order for it to be suitable for the manufacture of directly compressed tablets. The latter was explored during this study through the nanocoating of aqueous suspensions of Kraft softwood fibers with various polymers, using a layer-by-layer (LbL) self-assembly process.

The layer-by-layer (LbL) coating process is the sequential application of alternate polyelectrolytes or charged nanoparticles onto the surface of a charged substrate (Lvov et al., 1993). These ultrathin coatings can be functionalized for controlled drug delivery purposes (Ai et al., 2003; De Geest et al., 2006) or to adjust the properties of the coated substrate (Lu et al., 2007), and the properties of this coating depends on the nature of the molecules that make up the coating. It has been shown that colloidal SiO_2 is suitable for coating lignocellulose wood microfibers in order to improve the tensile strength of paper sheets made from these cellulose fibers, and cellulose fibers have also been coated with polymers in order to alter the surface properties of these fibers (Huang et al., 2005; Lu et al., 2007). This thus indicates that the LbL coating method might be a well suited technique to alter the properties of unmodified cellulose for making it suitable for use during direct compression. The aim of this study is to determine the feasibility of the LbL technique in coating cellulose fibers with polyelectrolytes commonly used in LbL coating and other biocompatible polymers in order to improve the flow, compression and tableting properties of cellulose fibers.

2. Materials and methods

2.1. Materials

Beaten, bleached (TCF) Kraft softwood fibers from Southern Pine (dried after beating) were supplied by International Paper Company, Bastrop, LA. Short damaged fibers were prepared by Wiley milling the dry pulp strips and passing it through a 60 mesh screen (resulted fiber length was 0.2 ± 0.1 mm). Fluorescein-5-isothiocyanate (FITC), cationic poly(dimethyldiallyl ammonium chloride) (PDDA; MW 200,000), anionic sodium poly(styrenesulfonate) (PSS; MW 70,000), polyvinylpyrrolidone (PVP, K30, MW ~ 40,000) and the charged polypeptides, gelatin type B (alkali processed or bovine gelatin; Bloom strength 225, MW 50,000–100,000) and chitosan (medium molecular weight), was purchased from Sigma–Aldrich (St. Louis, MO, USA). Microcrystalline cellulose USP/NF, Avicel® PH101 and PH102 were purchased from FMC Corporation (Newark, DE, USA). Milli-Q water with a resistivity of 18.2 MΩ/cm was used throughout this study in the preparation of the dissolution media, and all other reagents were analytical grade unless otherwise stated.

2.2. LbL nanocoating of cellulose fibers

Based on the negative charge on the suspended cellulose fibers, 1 g of the fibers were suspended in 100 ml of a PDDA solution (2 mg/ml in PBS buffer pH 5.8). The isoelectric point of PDDA is 12 and therefore has a net positive charge at pH 5.8. The suspension was then sonicated for 15 min, transferred to centrifuge tubes and centrifuged at 10,000 rpm for 5 min. The separated coated fibers were washed three times with PBS buffer. Zeta potential measurements indicated reversal to positive charge due to PPDA masking the negative drug particle surface charge. The particles were then resuspended in 100 ml of PSS solution (2 mg/ml at pH 5.8), stirred for 20 min to ensure coating, centrifuged, and then washed three times. At this pH, PSS carries a net negative charge because the isoelectric point of PSS is below 1.0. This completes the assembly of the first bilayer. When gelatin B was used in the assembling process, it was dissolved in the PBS pH 5.8 at a concentration of 2 mg/ml. It was layered with PDDA because it has a negative charge at pH 5.8 (isoelectric point, ~4–5). Due to the low solubility of chitosan at pH 5.8 it was dissolved in 0.1 M HCl. At this pH chitosan has a net positive charge. When PVP (2 mg/ml in 0.1 M HCl) was used in the coating it was layered with PSS. In each case at least four bilayers were applied to the cellulose particles.

2.3. Characterization of LbL nanocoating

Prior to polyion multilayer formation on the cellulose fibers, the coating procedure was elaborated on gold electrode resonators of 9-MHz quartz crystal microbalance (QCM; USI-Systems Inc., Kyoto, Japan). The resonators were immersed in the polyion solutions for 25 min, removed, and dried. The added mass and the coating thickness (ΔL) can be calculated from the frequency shift (ΔF), according to the Sauerbrey equation and using a special scaling. For the instrument used in this study, the calibration was ΔL (nm) = $0.017 \Delta F$ (Hz). These optimized assembly conditions were applied to the LbL nanocoating on the cellulose particles. To ensure the reversal of charge after each polyion coating, the zeta-potential of the suspended particles were measured with a zeta-plus photon correlation spectroscopy and microelectrophoresis instrument (Brookhaven Instruments, Holtsville, NY, USA). Since the coating with PVP depended more on hydrogen bonding than charge the layering of PVP with PSS was also followed by depositing the film on quartz slides (Yang et al., 2007). Before film preparation, the quartz slides were thoroughly cleaned by immersion in boiling H_2SO_4/H_2O_2 (70:30, v/v) for 30 min, followed by rinsing with deionized water and drying with a stream of pure N_2. The quartz slides were also modified before LbL deposition of PVP by coating with two PDDA/PSS layers. The UV–vis absorbance measurements were obtained with an Agilent 8453 UV-Vis spectrophotometer (Santa Clara, CA, USA).

2.4. Microscopic analysis

Scanning electron microscopy (SEM) studies were performed on samples that were affixed on carbon-taped stubs and thinly coated with Au/Pd. Both a Hitachi S570 and a Hitachi S-900 FESEM was used to photograph the samples (Hitachi High Technologies, Pleasanton, CA, USA). All micrographs were recorded with a crystal emission of 10 keV. Additional SEM micrograph analysis was conducted with automated image analysis routines available in ImageJ 1.42 imaging analysis software. Confocal laser scanning microscopy (model DMI RE2; Leica, Allendale, NJ, USA) and fluorescent spectrometry (Photon Technology International, Lawrenceville, NJ, USA) were used to visualize the LbL coating. For fluorescence, the cellulose particles were coated with FITC labeled PDDA (Ai et al., 2003).

2.5. Powder flow properties

Prior to making measurements all powder were dried under vacuum for at least 24 h. Angle of repose measurements was made by allowing powder samples to fall freely from a height of 45 mm onto a constant base with a diameter of 40 mm, through a glass funnel. The angle of repose was determined by taking photographs of the powder mound and measuring the angle formed between the horizontal surface of the base and the incline using ImageJ picture editing software. The Hausner ratio and Carr's index for each sample was determined by pouring a known weighed quantity of

powder, equal to approximately 2 g powder, into a graduated 50 ml cylinder. The initial powder volume (bulk volume) was measured after which the cylinder was tapped on a hard surface for 2 min (approximately 200 taps), or until the powder volume remained constant, and a second volume measurement (tapped volume) was made. The Hausner ratio was calculated as the ratio between the tapped and bulk densities of each sample, whereas the Carr's index was calculated using Eq. (1) (Carr, 1965):

$$C_{\%} = \frac{\rho_t - \rho_b}{\rho_t} \times 100\% \quad (1)$$

where ρ_t and ρ_b are the tapped and bulk densities respectively. All measurements were repeated five times for each sample.

2.6. Compaction properties

The powder samples were compacted into tablets with a Carver auto bench top press (Wabash, IN). The tablets had a diameter of 12 mm and weighed approximately 250 mg. Each powder was kept under pressure for 30 s before the pressure was removed. Six different compaction forces: 60, 120, 180, 240, 300 and 360 MPa were used. Before compaction, the powders were dried under vacuum for at least 24 h and afterwards the tablets were rested for 12 h before the tablet weight and dimensions were measured. Diametrical tablet hardness was measured with a Varian VK 200 tablet hardness test unit (Varian, Palo Alto, CA), and this enabled the calculation of the tensile strength (σ) (Fell & Newton, 1970):

$$\sigma = \frac{2P}{\pi D t} \quad (2)$$

where P is the crushing strength, D the diameter and t the thickness of the tablets. The brittle fracture index (BFI) of the tablets was calculated using the following equation

$$\mathrm{BFI} = 0.5\left[\left(\frac{\sigma}{\sigma_0}\right) - 1\right] \quad (3)$$

where σ is the tensile strength of the tablet without a hole and σ_0 the tensile strength of a tablet with a hole. A modified punch and die set with upper and lower sides having a hole and a pin at their centers permitted the formation of compacts with a centrally located hole (~1.0 mm diameter) that acted as a stress concentration defect during tensile testing. BFI values were calculated for tablets compacted to comparable tensile strength and porosity.

The porosity of tablets, ε, was calculated using Eq. (4).

$$\varepsilon = 1 - \frac{\rho_{\mathrm{tablet}}}{\rho_{\mathrm{true}}} \quad (4)$$

where ρ_{tablet} is the density calculated using the volume and weight of each tablet and ρ_{true} is the true density of the material measured using a Quantachrome Model MPY-2 helium displacement pycnometer (Quantachrome Corporation, Syosset, NY).

Compactibility plots of tensile strength versus porosity was analysed with the Ryshkewitch equation (Ryshkewitch, 1953)

$$\sigma = \sigma_0 e^{-b\varepsilon} \quad (5)$$

where ε is the tablet porosity and σ is the tablet tensile strength. The constant σ_0 is the maximum tensile strength at zero tablet porosity and b is an empirical constant that has been related to the pore distribution within a tablet (Roberts et al., 1995).

Heckel plots were constructed by plotting the natural log of the inverse of the compact porosity against the respective compaction pressures in accordance to the Heckel equation

$$\ln\left(\frac{1}{\varepsilon}\right) = KP + A \quad (6)$$

where K and A are slope and intercept, respectively, and P is the compaction pressure applied. Regression analysis was performed on the linear portion of each curve, and the slope value (K) obtained was converted to mean deformation, yield, pressure (P_y) using the relationship

$$P_y = \frac{1}{K} \quad (7)$$

The areas under the Heckel curves ($\mathrm{AUC_H}$) were calculated using TableCurve 2D and it was used as a measure of the extent of volume reduction that the material experienced over the entire compaction pressure range (60–360 MPa).

2.7. Disintegration time and dissolution testing

Tablets for the disintegration study were prepared to have similar solid fractions ($1-\varepsilon$) and tensile strengths. The disintegration test was performed according to the US Pharmacopoeia/National Formulary disintegration method using water at 37 °C and an Erweka GmbH apparatus (type 712, Erweka, Offenbach, Germany). The disintegration times reported are averages of five determinations.

Dissolution testing was performed on six tablets made from cellulose, nanocoated cellulose or MCC, and acetaminophen (APAP) powder mixtures. Tablets made from the powder mixtures that contained 30 and 60% (w/w) acetaminophen were used for the dissolution testing. Tablets prepared with acetaminophen concentrations of greater than 60% (w/w) were too brittle to handle, and were deemed not practically acceptable. The dissolution method for acetaminophen tablets from the United States Pharmacopoeia 2007 was followed (USP 2007), and dissolution apparatus 2 (the rotating paddle method) was used during the dissolution testing of these samples. A Varian VK 7000 dissolution apparatus (Palo Alto, CA) was used with 900 ml phosphate buffer USP (pH 5.8) as the dissolution media, made with potassium phosphate monobasic (KH_2PO_4) and sodium hydroxide (NaOH). The paddles were rotated at 50 rpm and 2.5 ml of dissolution media were withdrawn at predetermined time intervals, up to 2 h, and it was immediately replaced with an equal amount of fresh dissolution media. The amount of AAP in solution was calculated by determining the ultraviolet (UV) absorbance of the withdrawn solutions at a wavelength of 243 nm (USP 2007), and this value was converted to a concentration value using a calibration curve.

3. Results and discussion

3.1. Particle morphology

This paper reports the use of the LbL coating on small soft wood cellulose fibers and demonstrates the use of these nanocoated particles as a direct compaction tablet diluent. Direct compression is a process by which tablets are compressed directly from powder blends of the active ingredient and suitable excipients without pre-treatment by wet or dry granulation. Cellulose and especially MCC, purified partially depolymerized cellulose prepared by treating α-cellulose with mineral acids, is a diluent often used in direct compression. Examination of commercially available MCC powders reveals that many have similar particle morphology but they differ significantly in particle size. The SEM images in Fig. 1 show MCC particles that appear very rough, with many wrinkles and folds, irregular in shape, and with aspect ratios from 1.5 to 3 (Shangraw et al., 1987). Closer inspection of the surface reveals a crystalline powder composed of agglomerated porous microfibers (Fig. 1b). SEM and laser confocal fluorescent photomicrographs of the milled softwood cellulose fibers are shown in Fig. 2. Milling damaged the ends of the fibers but caused little wall separation of the porous microfibers (Lvov et al., 2006). The majority of the fibers were very short (0.2 ± 0.1 mm) with aspect ratios similar to that of the MCC

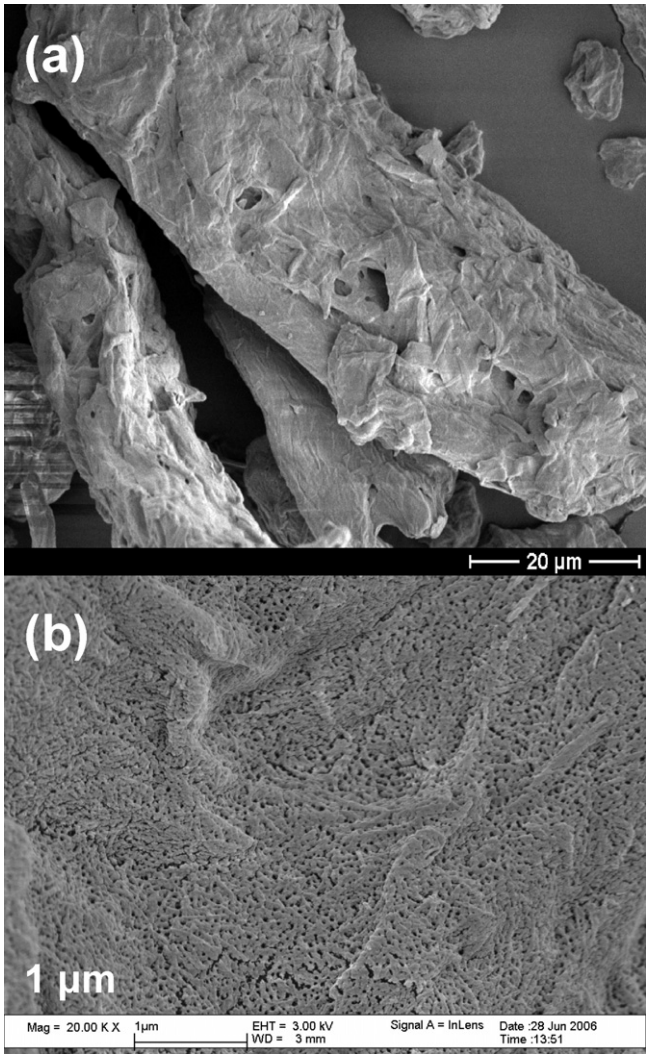

Fig. 1. SEM photomicrographs of (a) MCC (Avicel PH102) particle and (b) the surface of the MCC particle.

particles. Microscopically, Fig. 2a, the morphology and size of the uncoated cellulose and MCC particles appeared similar.

3.2. Characterization of the LbL nanocoating

The cellulose fibers were coated with polyelectrolytes commonly used in the LbL process (PDDA and PSS) and also GRAS and biocompatible polymers (gelatin, chitosan and PVP). The surface charge (ζ-potential) and change in surface charge is important for the LbL nanocoating process. The cellulose fibers had a negative potential of -30 ± 2.1 mV. The first precursor polyelectrolyte layers provided even coating and showed a change in surface potential with values of $+35 \pm 3.0$ mV for cationic PDDA and -27 ± 1.9 mV for anionic PSS. Overall, alternate ζ-potential values were observed for all multilayer films (Fig. 3). The results shown in Fig. 3 confirmed the LbL nanocoating of PDDA/PSS, PDDA/gelatin, PSS/chitosan orchitosan/gelatin in organized alternating layers. For each layer deposited, the underneath layer could have a different molecular distribution and conformation, which may explain the slight variations of the measured ζ-potential values for a specific polyelectrolyte when combined with different oppositely charged polyelectrolytes. SEM photomicrographs, Fig. 2b, also showed the coating because compared to uncoated particles smoother particle edges, and filled cracks and pores were observed after coating. Con-

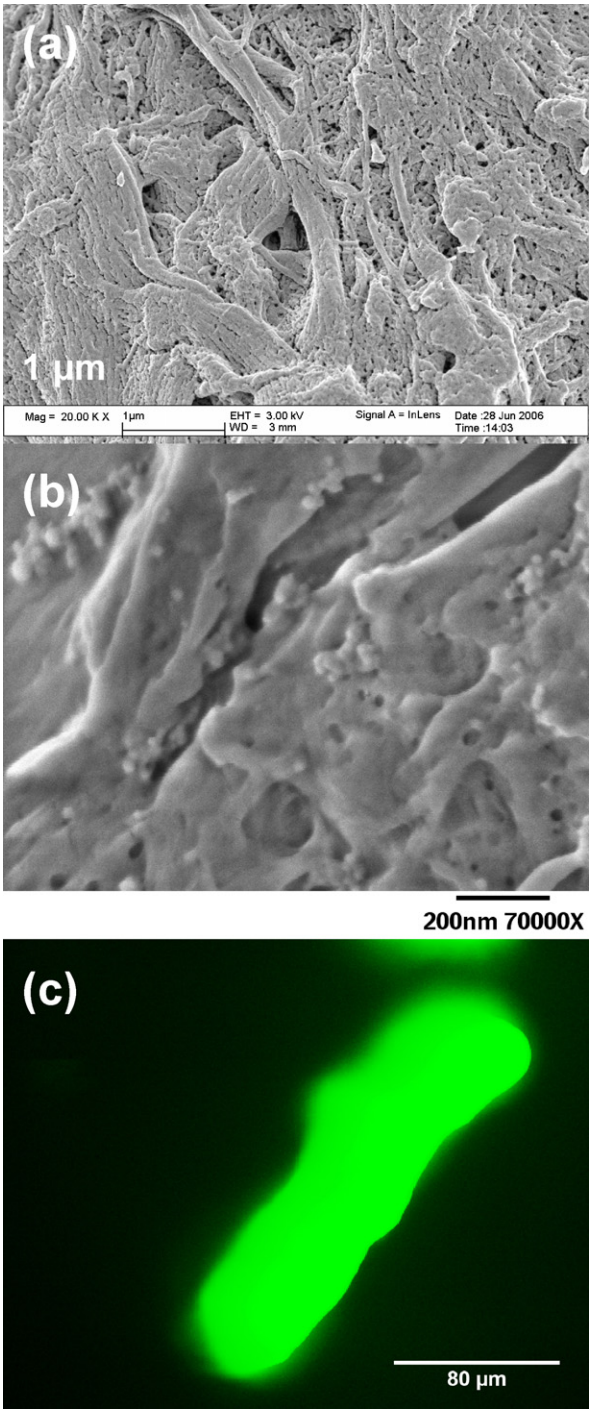

Fig. 2. SEM photomicrographs of the surface of (a) cellulose particle and (b) a cellulose particle coated with $(PDDA/(PSS/PVP)_3)$. (c) Laser confocal fluorescent image of a cellulose particle coated with labeled $(PDDA\text{-}FITC/PSS)_8$.

focal images, Fig. 2c, of the bright green fluorescence of microfibers coated with eight layers of labelled FITC-PDDA alternated with PSS also confirmed the uniform polymer nanocoating on the surface of the fibers. Confocal microscopy was used as a measurement to confirm the LbL coating.

The coating thickness was estimated from QCM measurements. A resonance frequency shift, Fig. 4, of the LbL nanocoated QCM-resonator enabled the calculation of the thickness of deposited polyelectrolyte multilayers. On the resonator each step of the PDDA/PSS polycation/polyanion deposition added approximately 2–5 nm thickness to the nanocoating thickness (Fig. 4). From this it

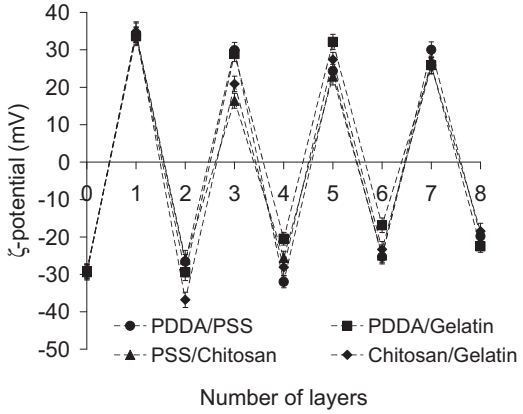

Fig. 3. Change in the cellulose particles ζ-potential during the LbL nanocoating.

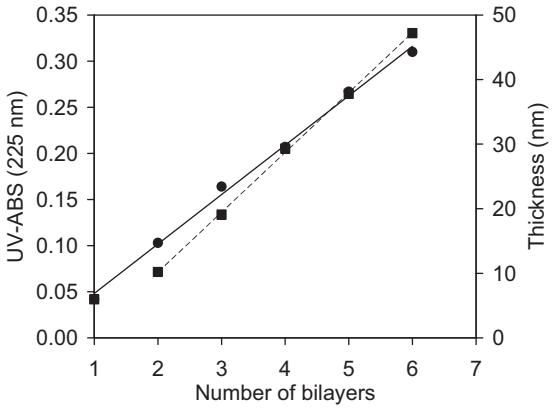

Fig. 5. (a) Monitoring of the LbL PSS/PVP assembly process by UV/Vis spectroscopy (λ = 226 nm) (solid line). (b) Thickness of PSS/PVP bilayers derived from QCM monitoring of resonance shifts on quartz resonators (broken line).

was estimated that the total thickness of the PDDA/PSS nanocoat was ~15 nm. This added about 0.15% to the total weight of the each fiber. Similarly the thickness of the PDDA/gelatin nanocoat was ~29 nm, the PSS/chitosan nanocoat ~25 nm and the chitosan/gelatin nanocoat ~64 nm. The 0.6% increase in weight for the chitosan/gelatin nanocoat was double that for the PDDA/gelatin and PSS/chitosan (0.3%), and four times that of the PDDA/PSS nanocoat. Together the QCM results showed that these ultrathin coatings added less than 1% to the weight of the cellulose fibers. This is significant because addition of these coatings by processes such as blending, granulation or spray coating would require significantly larger quantities of the polymers.

Since the adsorption of PVP depends on hydrogen bonding more than change interactions, the absorption of PSS/PVP bilayers were followed by UV spectroscopy at λ = 225 nm. This wavelength corresponds to absorbency of benzyl rings of PSS (Lvov et al., 1994). Since the deposition was done on both sides of the glass slide the increase in absorbance, Fig. 5, correspond to the absorbance value of double the number of bilayers deposited. There was a linear increase in absorbency with number of bilayers; therefore, the mass of the film was increasing linearly too. The thickness of the PSS/PVP layers deposited by the LbL technique was calculated from QCM data and Fig. 5 shows the film thickness versus number of bilayers. The average thickness of each PSS/PVP bilayer was estimated to be 9 ± 0.7 nm. Since the results in Fig. 4 showed that a single PSS layers is about 2–3 nm thick, each bilayer is composed mostly of PVP. The total thickness of the nanocoat containing PVP in three of the bilayers and on the outer surface was 30 nm which included

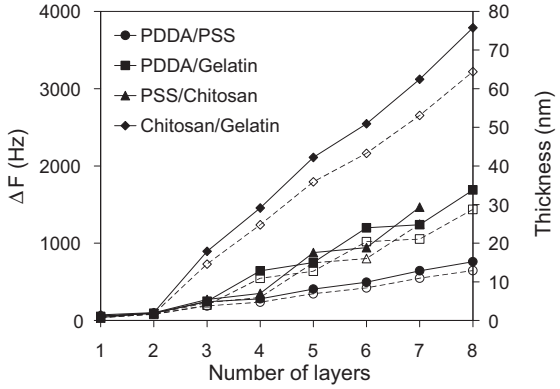

Fig. 4. QCM monitoring of resonance shifts by the subsequent nanoassembly of multiple layers on quartz resonators (solid lines and closed symbols) and thickness of layers relative derived from QCM data (broken lines and open symbols). Adsorption time is 25 min for every step.

the 2–3 nm thick PDDA precursor layer. This increased the weight of each particle by approximately 0.3%. These results demonstrate the successful self-assembling of a PSS/PVP nanocoat on the cellulose fibers.

3.3. Powder flow properties of nanocoated cellulose

The flow properties of powders are of critical importance in the production of tablets by the direct compression method. The powder flow properties of the nanocoated cellulose fibers are listed in Table 1. For powders that flow the angle of repose is often used to indicate differences in flow properties. Angles ≤25° corresponds to excellent flow while angles >50° indicates very poor flow. The uncoated cellulose fibers had an angle of repose of 64° indicating unsatisfactory flow. Although the angle of repose values, Table 1, indicated that the flow properties of the nanocoated powders were only passable (between 30 and 40°) it was similar to that of commercially available MCC powders (Geldart et al., 1990). According to Geldart's classification of powders a Hausner ratio of 1.96 of the uncoated cellulose powder means it is poorly flowable and difficult to fluidize (Geldart, 1973). The Hausner ratios of all the nanocoated powders were <1.25 indicating that they were non-cohesive with good flow, similar to that of Avicel PH102. Angle of repose and Hausner ratios was confirmed by the Carr's compressibility values listed in Table 1 (Hiestand, 2002). These powder flow property values indicated that LbL nanocoating changed the flow properties of the cellulose fibers from exceedingly poor to good. It also converted the cellulose fibers into powders that flowed as well or better than MCC powders. Powder flow was again tested on samples stored for 36 months at room temperature and the values obtained was within 5% of the original test results. This shows the stability or the coatings.

3.4. Compaction properties of nanocoated cellulose

Compaction studies, because they mimic the tableting process, were used to assess the mechanical properties of the nanocoated cellulose fibers. In Fig. 6 the change in tensile strength versus compaction pressure for the nanocoated cellulose fibers is shown. In this study this relationship was used to measure the tabletability of vacuum dried powders using zero-pressure measurements (Sun, 2008). Since at both low and very high pressures considerable deviations of the experimental data occur due to particle rearrangements and strain hardening a pressure range of 60–360 MPa was used (Sun, 2008). Within this pressure range both cellulose and MCC undergo plastic deformation of the primary particles that

Table 1
Compressibility and powder flow properties of the nanocoated cellulose particles. Type of flow was characterized according to Carr's compressibility values (Hiestand, 2002).

Nanocoating	Angle of repose (°)	Hausner ratio	$C_{\%}$	Type of flow
Uncoated cellulose	64	1.96	49	Exceedingly poor
PDDA/PSS	38	1.23	15	Good
PDDA/gelatin	38	1.16	17	Fair
PSS/chitosan	41	1.22	28	Poor
Chitosan/gelatin	38	1.18	20	Fair
PDDA + PSS (1:1)	37	1.17	15	Good
PSS/PVP	37	1.16	14	Good
Avicel PH101	41	1.32	24	Passable
Avicel PH102	36	1.17	14	Good

contributed predominantly to the formation of compacts (Doelker, 1993). In this study the MCC powders used as controls formed intact tablets within this compaction pressure range. The results in Fig. 6a show that cellulose fibers coated with a PSS/PVP nanocoat and tablets made from a 1:1 mixture of fibers with PDDA or PSS on the outer surface had the highest tensile strength over the entire compression range. The significantly higher tensile strength of the tablets containing PVP could be due to the excellent tablet binding properties of PVP (Horn and Ditter, 1982). In addition, a previous study has shown that when mixing oppositely charged LbL-treated pulps, then in addition to inter-fiber hydrogen bonding, the electrostatic interactions between positive and negative fibers provide stronger bonding in the paper (Zheng et al., 2006). The PSS/chitosan coated cellulose compacts had the lowest tensile strength at each compaction pressure. There was no significant difference between the compaction properties of the other nanocoated fibers and the MCC powders. Tensile strength was measured for samples stored for 36 months at room temperature and the values obtained was within 5% of the original test results for all the coated samples. This shows the stability of the coated cellulose fibers.

In powder compaction the observations of Heckel is often used to evaluate the stress of a material during compression (Heckel, 1961). In Fig. 6b the effect of compression on the porosity of the powder compacts is shown. With increasing pressure, the density of all the powder increased leading to decreasing porosity. Within the pressure range studied a near straight-line relationship (mean $R^2 = 0.994 \pm 0.003$) existed between $\ln[1/1(1-D)$ and P (Eq. (6)) for Avicel PH102, the PDDA/gelatin and PSS/PVP coated, and a 1:1 mixture of fibers with PDDA or PSS on the outer surface (Fig. 7). For these powders tablet density approached zero porosity faster. This meant that they undergo more permanent plastic deformation to more effectively eliminate pores. For these powders lower tablet porosity also resulted in larger areas of interparticulate bonding thus stronger tablets. Although linearity was not observed over the whole compression pressure range for the other nanocoated powders, linearity was seen for at least 60–240 MPa (mean $R^2 = 0.99 \pm 0.004$, Table 2). The mean yield pressure values calculated from the slope of the Heckel curve (Eq. (7)) (Table 2) show that, compared to Avicel PH102, the PSS/PVP coated fibers and a 1:1 mixture of fibers with PDDA or PSS on the outer surface undergo plastic deformation at a lower compaction pressure. The greater compactibility of these powders was also evident from the AUC_H values because the AUC_H for the PSS/PVP powder was 1.3 and the mixture of positive and negative particles 1.2 large than that of Avicel PH102. The mean yield pressure and AUC_H indicate that these two nanocoated powders were the most ductile materials. Except for the PSS/chitosan coated fibers that was the least ductile the yield pressures and AUC_H values of the other nanocoated cellulose fibers were comparable to that of the MCC powders.

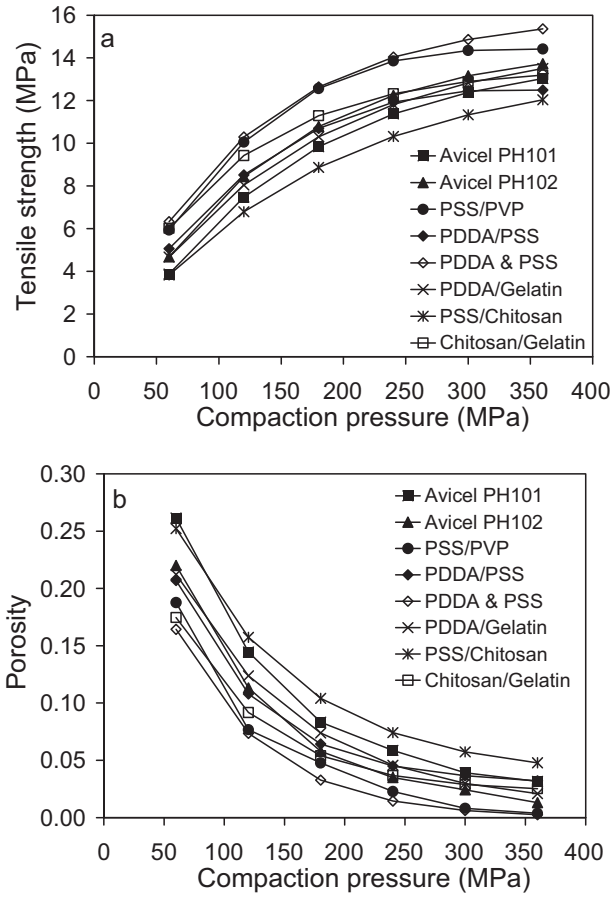

Fig. 6. Influence of LbL nanocoating on the (a) tensile strength and (b) porosity of cellulose compacts as a function of compaction pressure. Each nanocoat was composed of four bilayers of the polyelectrolytes which included a precursor PDDA layer or PDDA/PSS bilayer. For comparison the compaction properties of Avicel PH101 and PH102 are also shown.

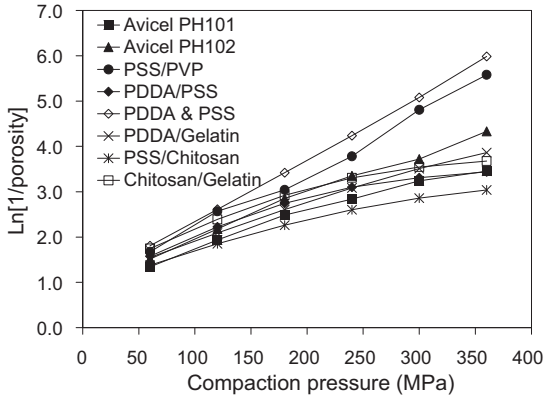

Fig. 7. Heckel plots for LbL nanocoated cellulose particles and Avicel PH101 and PH102.

Table 2
BFI values and the mechanical properties of coated cellulose particles derived from Heckel analysis. The AUC_H was calculated over the entire compaction pressure range of 60–360 MPa. Results for the uncoated cellulose particles is not shown because compacts laminated upon compression over the entire compaction pressure range.

Nanocoating	Compaction pressure range (MPa)	BFI[a]	P_y (MPa)	Heckel R^2	AUC_H
PDDA/PSS	60–240	0.11 ± 0.03	118	0.989	892
PDDA/gelatin	60–360	0.12 ± 0.02	129	0.995	835
PSS/chitosan	60–240	0.18 ± 0.02	147	0.987	699
Chitosan/gelatin	60–240	0.15 ± 0.03	115	0.990	879
PDDA + PSS (1:1)	60–360	0.11 ± 0.02	72	0.998	1157
PSS/PVP	60–360	0.09 ± 0.02	78	0.992	1073
Avicel PH101	60–300	0.08 ± 0.01	128	0.989	765
Avicel PH102	60–360	0.05 ± 0.01	108	0.991	897

[a] BFI were calculated for tablets compacted to comparable tensile strength and porosity (see Table 3).

Even though cellulose powders are generally compactible the stability of these compacts depends on the ability of the materials to relieve stresses without undergoing brittle fracture. For example the uncoated cellulose powders formed compacts but were not able to relieve stress rapidly enough and the tablets always capped or laminated. In this study BFI values (Eq. (3)) was used to measure the ability of compacts to withstand fracture (Hiestand, 1996). The BFI values (Table 2) for all the powders were <0.2 and except for the Avicel PH102 that had the smallest BFI value, the BFI values of all the other powders were not significantly different ($p < 0.05$). BFI values <0.2 indicated that all the compacts were able to relieve stresses sufficiently such that brittle fracture was not significant (Hiestand, 1996). This meant that tablets made with the nanocoated cellulose fibers were not likely to cap or laminate when compacted under the compaction pressures used in this study. In addition, according to Hiestand (1996) experience has also taught that when BFI values are <0.2, there will be no problem with fracture during tableting on a rotary press unless the bonding is very weak.

Compactibility can also be represented by a plot of tablet tensile strength versus porosity. In this study tensile strength versus porosity for the powders was plotted and the data were extrapolated using the exponential relationship shown in Eq. (5) (Ryshkewitch, 1953; Roberts et al., 1995). For all the materials, except the uncoated cellulose fibers that did not form intact compacts, the correlation coefficient of the non-linear regression, R^2, was >0.995. From these fits the maximum tensile strength at zero tablet porosity (σ_0) were extrapolated and the values are given in Fig. 8. The mean σ_0 for all the powders was 15 ± 0.3 MPa indicating no statistically significant difference ($p < 0.05$). This means that tablet tensile strength at a common porosity was approximately constant for all the nanocoated and MCC powders. The constant b in Eq. (5) has been related to the pore distribution within a tablet (Roberts et al., 1995; Sun, 2008; Sun and Grant, 2001). Lower values of b are characteristic of homogeneous pore distribution, whereas higher values of b are indicative of inhomogeneous porosity. The results in Fig. 8 show the b values for the materials used in this study. The average $b = 5.3 \pm 0.2$ (maximum 5.5 and minimum 5.0) is similar to that reported by others for MCC and indicate that in terms of tablet porosity, within the studied pressure range evaluated, the nanocoated cellulose produced compacts that were similar or better than MCC tablets. Although statistically not significant the b value for the PSS/PVP coated cellulose was the lowest and contributed most to the variance. Since b is the slope of the $\ln(\sigma)$ versus ε line, the lower b value corresponds to a slower increase in tensile strength as porosity is reduced.

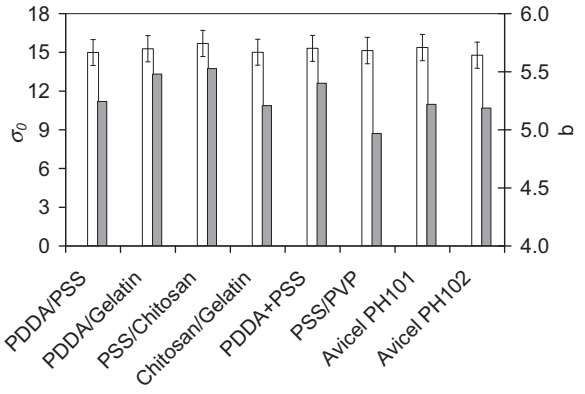

Fig. 8. Change in the compactibility parameters σ_0 (non-filled bars) and b (filled bars) for nanocoated cellulose fibers derived from the Ryshkewitch equation.

3.5. Disintegration of compacts

The disintegration times of tablets compressed to similar solid fractions (0.94–0.96) and tensile strengths (11–13 MPa) are listed in Table 3. The uncoated cellulose compacts disintegrated the fastest because it formed very poor compacts that capped and laminated. Compacts of both Avicel PH101 and Avicel PH102 did not disintegrate within 100 min because although MCC is a strong binder and good wicking agent it does not swell and when compacted on its own, does not disintegrate (Kumar et al., 2002). Tablets made with the PDDA/PSS nanocoated fibers and a 1:1 mixture of fibers with PDDA or PSS on the outer surface also did not disintegrate within 100 min. Compared to these and the MCC compacts tablets prepared with the LbL nanocoated cellulose fibers coated with gelatin, chitosan and PVP disintegrated within 50 min. Although the disintegration times was faster for compacts made with these powders tensile strength and porosity values still indicate that these powders are strong binders. Since, the tensile strength and solid fraction values obtained for tablets were comparable it appears that the difference seen in the disintegration times must be due to the wettability of the nanocoating (Wu et al., 2007). Contact angle measurements of the coated quartz resonators used for QCM analysis indicated that PDDA or PSS coating had contact angles between 30 and 40° while water spread completely on those coatings having chitosan, gelatin or PVP on the surface. This would make it easier for water to access and enter the compacts which in turn would promote disintegration.

In order to determine if the nanocoatings have an influence on the release rate of a drug from tablets, dissolution tests were performed on tablets prepared from powder mixtures between coated cellulose fibers or MCC and APAP. The dissolution of tablets containing 30% and 60% APAP were tested. APAP is poorly released from the tablets prepared from unmodified cellulose. This is due to the fact that these tablets did not completely disintegrate during the dissolution analysis which slowed down the release of the drug from these tablets. However, it was seen that the dissolution profiles of the acetaminophen tablets made from coated fibers, and containing both 30% and 60% (w/w) APAP, were similar to the dissolution profiles of the tablets made with the MCC powder. Similarity was confirmed by f_2 calculations (SUPAC-IR, 1995). SUPAC-IR suggest

Table 3
Disintegration times of tablets compacted to comparable tensile strength and porosity.

Nanocoating	Compaction pressure (MPa)	Tensile strength (MPa)	Solid fraction (%)	Disintegration time (min)
Cellulose	360	–	95.1	4 ± 1
PDDA/PSS	240	11.4	95.5	>100
PDDA/gelatin	240	11.9	95.4	35 ± 7
PSS/chitosan	360	11.8	95.2	>100
Chitosan/gelatin	180	12.0	94.6	42 ± 6
PDDA + PSS (1:1)	180	11.3	96.0	>100
PSS/PVP	180	12.6	95.2	26 ± 5
Avicel PH101	240	11.4	94.1	>100
Avicel PH102	180	10.8	94.2	>100

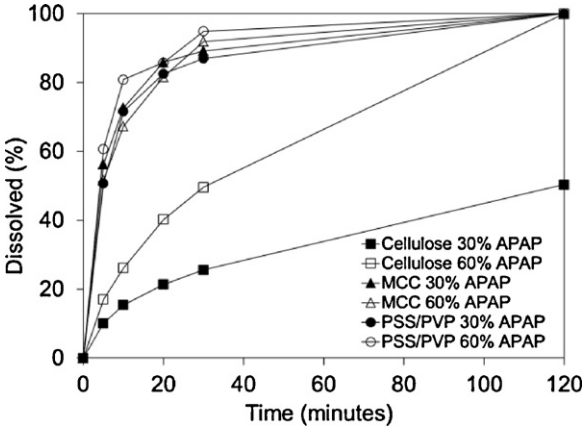

Fig. 9. Dissolution profiles for APAP tablets prepared from blends of the drug and uncoated lignocellulose, lignocellulose LbL coated with PSS/PVP and uncoated MCC.

that similarity between two dissolution profiles be concluded if f_2 is between 50 and 100, where 50 represents an average 10% difference at all sampling time points and 100 is the upper bound of f_2 when the distance at all sampling time points is 0. The results from the dissolution tests for cellulose fibers coated with PSS/PVP compared to uncoated fibers and MCC are shown in Fig. 9.

4. Conclusion

The results for the compactibility of nanocoated soft wood microfibers obtained in this study showed that LbL self-assembling of nano thin polymer layers on cellulose fibers can be used to produce cellulose based directly compactible tablet diluents. The powder flow properties and tableting indices of compacts compressed from these nanocoated microfibers were similar or better than that of directly compactible MCC powders. Cellulose microfibers coated with four PSS/PVP bilayers had the best compaction properties while still producing tablets that were able to absorb water and disintegrate and for a model drug, APAP, produced tablets with similar dissolution profiles. Although the mechanism for improve compactibility of the coated cellulose fibers is not completely understood it is thought that a combination of better flow, better compression, and the addition of a nanocoat of the polymers that act as a binder all contributes to the improved performance of the nanocoated fibers when compared to MCC.

The advantages of using LbL nanocoating rather than traditional pharmaceutical coating processes are that it allows control of the molecular properties of the surface and the thickness of the coat to within a few nanometers, and that it add less than 1% to the weight of the fibers. Although the LbL coating process involved milling, suspension, centrifuging (or filtering) and drying of coated fibers, this process is potentially friendlier to the environment because it uses biocompatible and degradable materials and does not involve acid-catalyzed hydrolysis and neutralization of depolymerized cellulose.

Acknowledgements

We are grateful to the University of Wisconsin, the North-West University, Louisiana Tech University and the National Research Foundation of South Africa (NRF) for research support. We want to thank Louwrens R. Tiedt from the Laboratory for Electron Microscopy, Faculty of Natural Sciences, North-West University, Potchefstroom, South Africa and Joseph Heintz from the Biological and Biomaterials, Preparation, Imaging and Characterization (BBPIC) laboratory at UW – Madison, Animal Sciences, for their assistance with the SEM and confocal microscopy.

References

Ai, H., Jones, S.A., De Villiers, M.M., Lvov, Y.M., 2003. Nano-encapsulation of furosemide microcrystals for controlled drug release. J. Control. Release 86, 59–68.
Aulton, M.E., 2000. Cellulose, powdered. In: Kibbe, A.H. (Ed.), Handbook of Pharmaceutical Excipients. Pharmaceutical Press, London, pp. 107–109.
Carr Jr., R.L., 1965. Classifying flow properties of solids. Chem. Eng. 72, 69–72.
Chuayjuljit, S., Su-Uthai, S., Tunwattanaseree, C., Charuchinda, S., 2008. Preparation of microcrystalline cellulose from waste-cotton fabric for biodegradability enhancement of natural rubber sheets. J. Reinf. Plast. Compos. 28, 1245–1254.
De la Luz Reus Medina, M., Kumar, V., 2006. Evaluation of cellulose II powders as a potential multifunctional excipient in tablet formulations. Int. J. Pharm. 322, 31–35.
De la Luz Reus Medina, M., Kumar, V., 2007. Modified cellulose II powder: preparation, characterization, and tableting properties. J. Pharm. Sci. 96, 408–420.
De Geest, B.G., Déjugnat, C., Verhoeven, E., Sukhorukov, G.B., Jonas, A.M., Plain, L., Demeester, J., De Smedt, S.C., 2006. Layer-by-layer coating of degradable microgels for pulsed drug delivery. J. Control. Release 116, 159–169.
Doelker, E., 1993. Comparative compaction properties of various microcrystalline cellulose types and generic products. Drug Dev. Ind. Pharm. 19, 2399–2471.
Fell, J.T., Newton, J.M., 1970. Determination of tablet strength by the diametral-compression test. J. Pharm. Sci. 59, 688–691.
Geldart, D., 1973. Types of gas fluidization. Powder Technol. 7, 285–292.
Geldart, D., Mallet, M.F., Rolfe, N., 1990. Assessing the flowability of powders using angle of repose. Powder Handling Process. 2, 341–346.
Heckel, R.W., 1961. Density–pressure relations in powder compaction. Trans. Am. Inst. Min. Metall. Pet. Eng. 221, 671–675.
Hiestand, E.N., 1996. Rationale for and the measurements of tableting indices. In: Alderborn, G., Nystrom, C. (Eds.), Pharmaceutical Powder Compaction Technology. Marcel Dekker, New York, pp. 219–244.
Hiestand, E.N., 2002. Mechanical and Physical Principles for Powders and Compacts, 2nd ed. SSCI, West Lafayette.
Horn, D., Ditter, W., 1982. Chromatographic study of interactions between poly(vinylpyrrolidone) and drugs. J. Pharm. Sci. 71, 1021–1026.
Huang, J., Ichinose, I., Kunitake, T., 2005. Nanocoating of natural cellulose fibers with conjugated polymer: hierarchical polypyrrole composite materials. Chem. Commun. 13, 1717–1719.
Kumar, V., De la Luz Reus-Medina, M., Yang, D., 2002. Preparation, characterization, and tabletting properties of a new cellulose-based pharmaceutical aid. Int. J. Pharm. 235, 129–140.
Lindner, H., Kleinebudde, P., 1994. Use of powdered cellulose for the production of pellets by extrusion spheronization. J. Pharm. Pharmacol. 46, 2–7.
Lvov, Y., Ariga, K., Kunitake, T., 1994. Layer-by-layer assembly of alternate protein/polyion ultrathin films. Chem. Lett. 12, 2323–2326.
Lvov, Y., Decher, G., Möhwald, H., 1993. Assembly, structural characterization, and thermal behavior of layer-by-layer deposited ultrathin films of poly(vinyl sulfate) and poly(allylamine). Langmuir 9, 481–486.

Lvov, Y.M., Grozdits, G.A., Eadula, S., Zheng, Z., Lu, Z., 2006. Layer-by-layer nanocoating of mill broken fibers for improved paper. Nord. Pulp. Paper Res. J. 21, 552–557.
Lu, Z., Eadula, S., Zheng, Z., Xu, K., Grozdits, G., Lvov, Y., 2007. Layer-by-layer nanoparticle coating on lignocellulose wood microfibers. Colloids Surf. A 292, 56–62.
McCormick, D., 2005. Evolution in direct compression. Pharm. Technol. 4, 52–62.
Peck, G.E., Baley, G.J., McCurdy, V.E., Banker, G.S., 1989. Tablet formulation and design. In: Lieberman, H.A., Lachman, L., Schwartz, J.B. (Eds.), Pharmaceutical Dosage Forms: Tablets. Marcel Dekker Inc., New York, pp. 108–110.
Roberts, R.J., Rowe, R.C., York, P., 1995. The relationship between the fracture properties, tensile strength and critical stress intensity factor of organic solids and their molecular structure. Int. J. Pharm. 125, 157–162.
Ryshkewitch, E., 1953. Compression strength of porous sintered alumina and zirconia: 9th communication to ceramography. J. Am. Ceram. Soc. 36, 65–68.
Shangraw, R.F., Wallace, J.W., Bowers, F.M., 1987. Morphology and functionality in tablet excipients for direct compression. Pharm. Technol. 11, 136–143.
Stupińska, H., Iller, E., Zimek, Z., Wawro, D., Ciechańska, D., Kopania, E., Palenik, J., Milczarek, S., Steplewski, W., Krzyzanowska, G., 2007. An environment-friendly method to prepare microcrystalline cellulose. Fibres Text. East. Eur. 15, 167–172.
Sun, C.C., 2008. Mechanism of moisture induced variations in true density and compaction properties of microcrystalline cellulose. Int. J. Pharm. 346, 93–101.
Sun, C.C., Grant, D.J.W., 2001. Effects of initial particle size on the tableting properties of L-lysine monohydrochloride dihydrate powder. Int. J. Pharm. 215, 221–228.
SUPAC-IR, Guidance for Industry, 1995. Immediate Release Solid Oral Dosage Forms; Scale-up and Postapproval Changes: Chemistry, Manufacturing, and Controls; In Vitro Dissolution Testing; In Vivo Bioequivalence Documentation. Center for Drug Evaluation and Research, Food and Drug Administration, November.
Wu, T., Sun, Y., Li, N., De Villiers, M.M., Yu, L., 2007. Inhibiting surface crystallization of amorphous indomethacin by nanocoating. Langmuir 23, 5148–5153.
Yang, S., Zhang, Y., Zhang, X., Guan, Y., Xu, J., Zhang, X., 2007. From cloudy to transparent: chain rearrangement in hydrogen-bonded layer-by-layer assembled films. ChemPhysChem 8, 418–424.
Zheng, Z., McDonald, J., Khillan, R., Su, Y., Shutava, T., Grozdits, G., Lvov, Y.M., 2006. Layer-by-layer nanocoating of lignocellulose fibers for enhanced paper properties. J. Nanosci. Nanotechnol. 6, 624–632.